Modeling tracheobronchial clearance of nanoparticles with variable size and geometry

Robert Sturm

Department of Chemistry and Physics of Materials, University of Salzburg, Salzburg, Austria

Correspondence to: Dr. Robert Sturm. Brunnleitenweg 41, 5061 Elsbethen, Austria. Email: sturm_rob@hotmail.com.

Background: Nanoparticles transported in the ambient atmosphere are generally characterized by a great variety of shapes and aerodynamic diameters adopting values less than 100 nm. According to numerous experimental und theoretical studies such particulate objects have the ability to enter the respiratory tract, where they may deposit in the airway tubes and alveolar structures. After their deposition, the particles are subjected to an innate defence system containing various clearance mechanisms. In this contribution, tracheobronchial clearance of nanoparticles settled on the airway walls is investigated theoretically.

Methods: Tracheobronchial clearance of nanoparticles inhaled by healthy adults under sitting breathing conditions was simulated by assuming a stochastic architecture of the lung and a continuous mucus transport from the terminal bronchioles to the trachea. The clearance process taking place in single bronchial and bronchiolar airways was subdivided into a fast phase with a total clearance time of less than 24 h and a slow phase with a duration of 25 to 100 d. Theoretical clearance curves and 24-h retention values were computed for spheres as well as cylindrical particles with diameters varying between 1 and 50 nm and aspect ratios ranging from 0.001 to 1,000.

Results: For nanospheres with diameters varying between 1 and 50 nm the theoretical model predicts 24-h retention values ranging from 81.0% to 86.9%. In the case of nonspherical particles, 24-h retention exhibits a clear dependence on aspect ratio. Therefore, platelets with aspect ratios between 0.1 and 0.001 are retained in the airways by 84.2% to 87.0%, whereas tubes with aspect ratios between 10 and 1,000 produce retention values ranging from 72.7% to 86.7%. Hypothetical clearance curves allow a strict distinction between fast and slow clearance phase.

Conclusions: Based on the theoretical results presented in this study, it may be concluded that thin nanoplatelets, nanospheres and long nanotubes are commonly characterized by remarkable differences with regard to their clearance in the tracheobronchial airways. Whilst nanoplatelets are preferably cleared by transcellular transport mechanisms, nanotubes are mainly removed from the tubular structures by mucociliary transport.

Keywords: Nanoparticle; deposition; mucociliary clearance; slow bronchial clearance; 24-h retention

Received: 02 March 2020; Accepted: 21 January 2021; Published: 25 June 2021.

doi: 10.21037/jphe-20-16

View this article at: http://dx.doi.org/10.21037/jphe-20-16

Introduction

By definition, nanoparticles represent very small objects with at least one spatial dimension adopting a size of less than 100 nm (1-10). In the ambient atmosphere, nanoparticles can be mainly found within the large group of 'bioaerosols' (e.g., viruses, bacteria, cell fragments). They also include ultrafine dusts produced by different mechanical procedures (e.g., milling, abrasion) as well as various particles originating from incomplete combustion processes [e.g., diesel particulate matter (DPM), soot] (11-15). In general, nanoparticles like those mentioned above are usually marked by geometries, which may significantly deviate from ideal spherical shape. Whilst small bioaerosols and dust particles preferentially adopt tubular or platelet-like geometries, diesel exhaust particles and soot chiefly occur as irregularly shaped aggregates containing a high number of nanoscopic components (11-20). All these particulate objects have in common that they may be taken up into the human body by inhalation. Depending on their size and shape nanoparticles show either a preference to deposit in the upper lung regions or a predilection to settle in the central to peripheral structures of the respiratory tract (21-29).

Immediately after their deposition in the different parts of the human respiratory tract nanoparticles are subjected to an innate defence system including a high variety of clearance mechanisms. In the tracheobronchial tree, fast clearance represented by the so-called 'mucociliary escalator' can be distinguished from a slow clearance phase, which seizes all those particulate objects not captured on the mucus layer (30-40). According to the present knowledge slow bronchial clearance includes the temporary storage of particles in the periciliary liquid, processes of transcytosis and extracellular transport as well as the uptake and removal of particulate mass by airway macrophages (30-35). Whilst mucociliary clearance is mainly finished within the first 24 hours after aerosol exposure, slow clearance mechanisms are thought to adopt half-times between 1 and 20 days, so that main particle masses seized by these processes are removed from the tracheobronchial tree after 5 to 100 days (*Figure 1*) (30-40).

In the nearer past, tracheobronchial clearance in the human respiratory tract stood in the focus of a multitude of experimental and theoretical studies (30-44). As a main result, it could be demonstrated that the fractions of fast and slowly cleared particles depend on the size, the geometry, and the physical density of the inhaled particulate material. According to numerous model computations, small spherical particles are cleared much slower from single bronchial and bronchiolar structures than large tubular or platelet-like objects. Whilst the spheres represent ideal targets for temporary storage in the periciliary liquid and transcellular dislocation processes, thin platelets with large diameters and long tubes cannot be handled by the epithelial cells in the same way and thus preferentially undergo a transport on the mucus layer (40-45).

In the study presented here, tracheobronchial clearance behaviour of nanoparticles with different sizes and geometries was submitted to a detailed theoretical investigation. For this purpose, spheres with a diameter of 1, 10, and 50 nm as well as cylindrical objects with same diameters and aspect ratios ranging from 0.001 (extremely thin platelets) to 1,000 (extremely long tubes/fibers) were generated. Tracheobronchial clearance of these particles was modelled for healthy adult subjects, who had inhaled respective aerosols under sitting breathing conditions (46). The study can be evaluated as innovative insofar as:

- ❖ It theoretically deals with a great variety of nanoparticles, which in very similar form also occur in nature;
- ❖ It presents new results concerning the removal of particulate mass from the tracheobronchial tree;
- ❖ It once more underlines the significance of particle geometry in association with theoretical lung modeling.

Methods

Main features of the clearance model

Since the mathematical approach used in this contribution has been already described in numerous preceding papers (30-45), only those features most salient for the understanding of the model will be outlined in this section. In principle, the related computer program includes a stochastic architecture of the human respiratory tract, where geometric parameters of airways (diameters, lengths, branching angles) belonging to a specific lung generation are normally distributed. For each bronchial and bronchiolar tube of the airway tree, morphometry is determined by application of parameter-related probability density functions on the one hand and the random number concept on the other (38,39). In order to obtain a reliable approximation of the mucus transport on the epithelial surface of the airway tubes (mucociliary clearance), it is assumed that the luminal side of the entire tracheobronchial tree is uniformly covered with a mucus blanket, which is marked by a constant transport velocity within each tubular element. In addition, the mucus layer of a given airway tube is characterized by constant thickness due to equal mucus production over the whole length of the bronchial or bronchiolar structure. Based upon an experimentally measured tracheal mucus velocity (TMV) of 15 mm/min and mucus thickness of 27 µm, mucus dynamics in the following airway generations are computed by using (I) an exponential function describing the development of mucus thickness from the main bronchi to the terminal bronchioles and (II) a downscaling procedure involving the stochastic airway morphometry described above. According

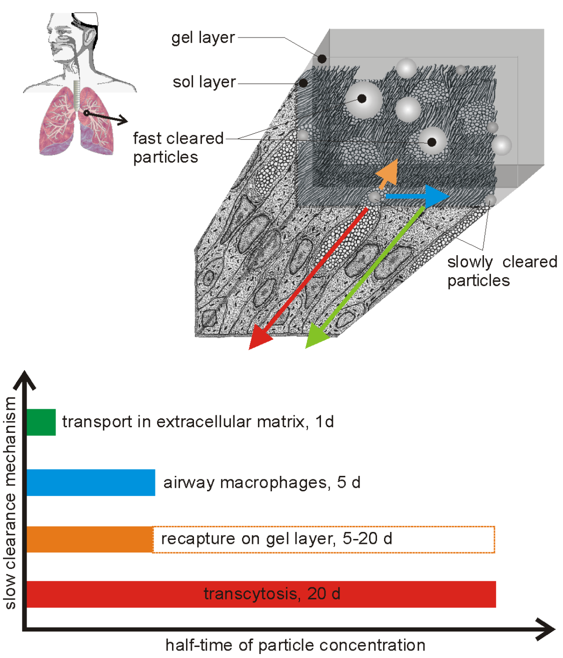

Figure 1 Histological organization of the bronchial/bronchiolar airway epithelium and its cover by the mucus blanket consisting of the highly viscous gel layer and the watery sol layer (periciliary liquid). Whilst particles captured on the gel layer are commonly removed by fast mucociliary clearance, particles reaching the sol layer undergo slow bronchial clearance. Regarding nanoparticles four different clearance mechanisms with half-times of particle concentrations ranging from 1 to 20 d can be distinguished.

to the model, respective mucus velocities determined for peripheral bronchiolar airways (generation 20) are four to five orders of magnitude lower than those measured in the trachea (30-40).

Theoretical approximation of slow bronchial clearance is carried out by determination of the slow clearance fraction (f_s) in a first step. This fraction includes all those particles settled on the epithelial walls, which are captured by clearance mechanisms beyond the mucociliary escalator. According to previous investigations, the number of slowly cleared particles mostly depends upon particle size, but is also related to the physical density and the geometry of the particulate objects. It is assumed that deposited particles have to pass the mucus blanket (by sedimentation or via discontinuities) and reach the so-called periciliary liquid in order to undergo slow bronchial clearance. Thereby, four independent mechanisms of this clearance phase can be distinguished: (I) re-transfer of particles from the periciliary liquid to the mucus layer due to cilia activity, (II) uptake of particles by epithelial cells with temporary storage and transcytosis, (III) uptake of particulate masses by airway macrophages, (IV) fast transport of particles to the blood capillaries via the extracellular matrix. All these mechanisms are characterized by half-times of the related particle concentrations ranging from 1 to 20 days (40-46). This results in durations of slow bronchial clearance varying between 5 and 100 days. Slow bronchial clearance mechanisms are assumed to exhibit an independence of the site within the tracheobronchial tree.

Definition of model parameters

Model computations were carried out under the assumption of a respiratory tract belonging to a male adult (FRC: 3,300 cm^3). For the deposition and subsequent clearance simulations, unit-density nanoparticles (1 g/cm^3) with spherical or cylindrical diameters of 1, 10, and 50 nm were used. Besides objects with ideal spherical geometry also cylindrical platelets with aspect ratios ranging from 0.001 to 0.1 as well as cylindrical fibers with aspect ratios ranging from 10 to 1,000 were included in the modelling procedure. Inhalation of the respective particle-loaded aerosols was supposed to take place under sitting breathing conditions [tidal volume: 750 cm^3, breath-cycle time: 4.5 s, breath-hold: 1 s (46)] and inhalation of the air through the nose. Clearance of single particles was expressed by calculation of retention values (24-h retention) on the one hand and the simulation of time-dependent clearance curves on the other.

Results

Dependence of retention values on particle size and shape

Retention values (i.e., ratios between particle numbers retained in the airways and particle numbers taken up into the tracheobronchial tree during inhalation) are summarized in *Figure 2*. Therefore, 24-h retention of nanoparticles with a spherical/cylindrical diameter of 1 nm generally ranges from 86.6% to 87.0%, whereby ideal spheres produce a value of 86.9%, platelets are characterized by values of 86.9% to 87.0% and fibers exhibit values of 86.6% to 86.7%. In the case of nanoparticles adopting a diameter of 10 nm, 24-h retention is marked by values ranging from 82.7% to 86.8% (spheres: 85.8%, platelets: 86.2–86.8%, fibers: 82.7–84.0%), whereas for a particle diameter of 50 nm this parameter amounts to 72.7 to 86.5% (spheres:

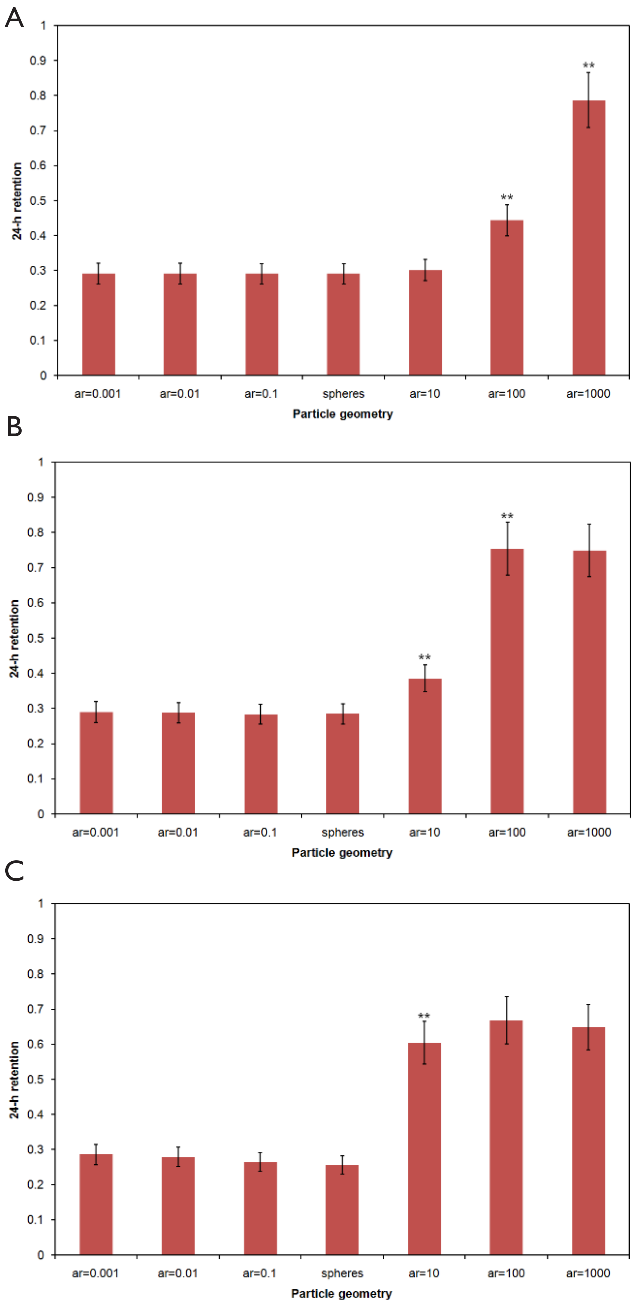

Figure 2 Twenty-four-h retention values (mean values +/− standard deviations) of nanoparticles with different diameter and aspect ratios (ar). (A) particles measuring 1 nm in diameter; (B) particles with a diameter of 10 nm; (C) particles with a diameter of 50 nm (**, P<0.001).

81.0%, platelets: 84.2–86.5%, fibers: 72.7–77.1%; *Figure 2*).

Retention values computed 10 days after particle exposure show very similar tendencies as 24-h retentions. Nanoparticles with a diameter of 1 nm are distinguished by 10-d retentions ranging from 0.0% to 37.7%. In the case of nanoparticles adopting diameters of 10 nm, this parameter amounts to 0.0% to 33.1%, whereas for nanoparticles with a diameter of 50 nm clearance simulation provides values varying between 0.0% and 23.1%.

Clearance curves modelled for single particle categories

Clearance curves describing short-term and long-term behaviour of nanoparticle removal from the tracheobronchial tree are summarized in *Figure 3*. With regard to nanoparticles with a diameter of 1 nm, total clearance times extracted from the functions generally range from 6 to 62 d. In the case of nanoparticles adopting a diameter of 10 nm, duration of tracheobronchial clearance varies between 6 and 39 d. Concerning nanoparticles measuring 50 nm in diameter, total clearance time commonly ranges from 5 to 26 d.

Discussion

Based on the results presented in this study it may be concluded that nanoparticles are characterized by highly specific clearance behaviour. In general, overall velocity and related duration of tracheobronchial clearance depends upon two particle parameters, namely the size and the geometry of the studied particulate objects. This means that nano-scale platelets with minimal thickness are cleared with an efficiency, which significantly differs from that of larger fibers with extreme length. The results summarized in *Figures 2* and 3 are largely confirmed by other theoretical studies provided by the author (30-45). In the case of spherical particles, also experimental confirmation of the model predictions is given, because it was found that ultrafine particles (<100 nm) may be removed from the epithelial surface via the extracellular matrix filling the caps between two neighbouring cells. This diffusional transport is remarkably accelerated with decreasing particle size and may result in an evacuation of particulate mass towards the

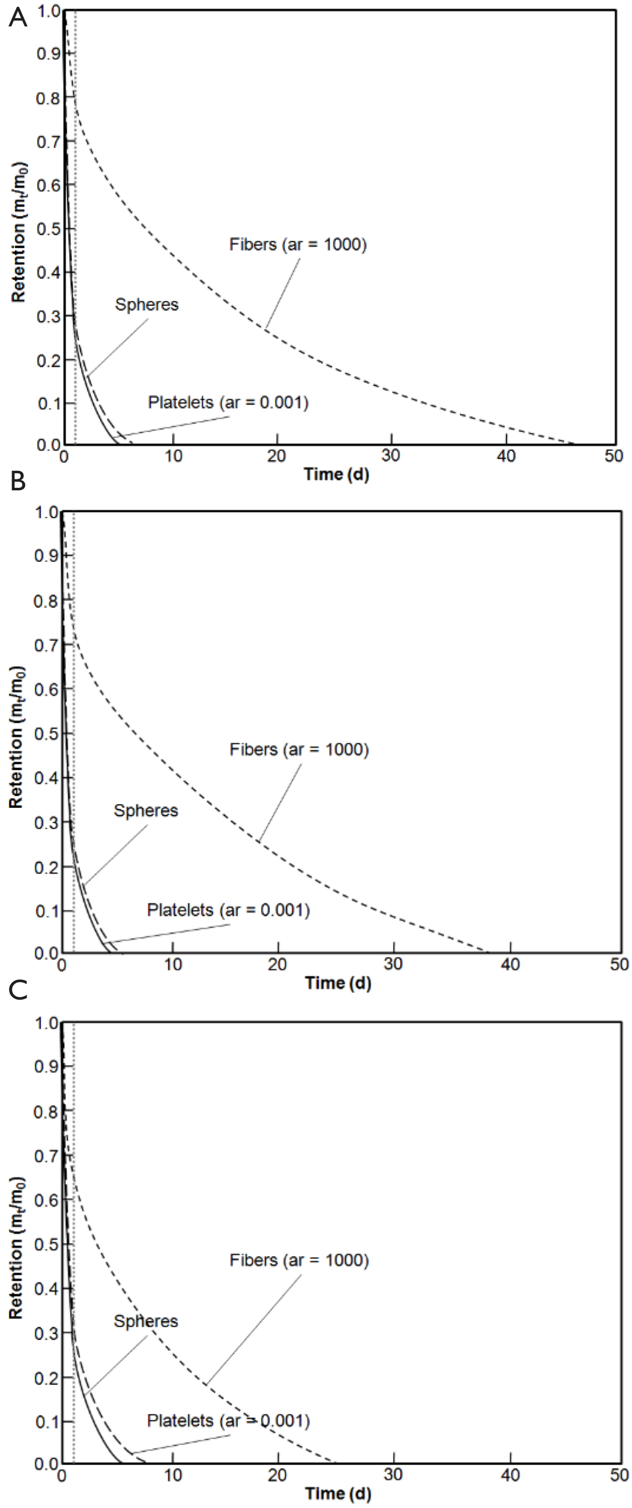

Figure 3 Clearance curves of nanoparticles with different geometries [very thin platelets (ar=0.001), spheres, extremely long fibers (ar=1,000)]. (A) Particles measuring 1 nm in diameter; (B) particles with a diameter of 10 nm; (C) particles with a diameter of 50 nm.

blood capillaries within several minutes to hours (41,42). For the other slow bronchial clearance mechanisms introduced in this contribution, only further theoretical data are available hitherto, whereas comparable results of targeted experiments are still very sparse (40-45).

In general, it may be noticed that tracheobronchial clearance of nano-scale particles differs from that of micro-scale particles in several aspects. Since slow bronchial clearance performs a continuous rise with declining particle diameter (40-45), nanoparticles produce much higher fractions of slowly cleared mass than microparticles [note: particles with a geometric diameter of more than 6 μm do not produce any slow clearance fraction at all (30-40)]. On the other hand, nanoparticles undergo an additional removal through the extracellular matrix representing an effective barrier for most particulate objects that belong to the micrometer scale (40-45). Summing up all these considerations, total tracheobronchial clearance times of nanoparticles on the one side and microparticles on the other are characterized by rather similar values. According to numerous histological investigations it has to be assumed that tracheobronchial clearance exhibits great differences between the upper, central and peripheral airways. Since the number of goblet cells and subepithelial glands is successively diminished from airway generation 1 to 20, efficiency of the mucus transport is marked by a similar decline. Hence, larger particles deposited in small ciliated airways are captured by slow clearance mechanisms to a higher extent than predicted by most models (41,46).

The influence of particle geometry on the distribution of fast and slowly cleared particulate masses was already predicted in many previous papers (40-45,47-50). Whilst ultrathin nanoplatelets already approach molecular size and thus undergo a kind of molecular transport in the different cell layers, ultralong nanofibers partly adopt the aerodynamic and clearance behaviour of micro-scale particles being marked by prolonged intracellular storage phases (40-45). From a pharmacological state of view, medicals administered to the respiratory tract in the form of nanospheres are mainly deposited in the upper and central airways, where they have the ability to reach the lung-associated blood vessels within a rather short period of time (47-50).

A retrospection on the results of this contribution allows the conclusion that the prediction and measurement of nanoparticle clearance may be an essential field of medical research in nearer future, so that numerous studies dealing with this question should follow in the next years.

Acknowledgments

Funding: None.

Footnote

Data Sharing Statement: Available at http://dx.doi.org/10.21037/jphe-20-16

Conflicts of Interest: The author has completed the ICMJE uniform disclosure form (available at http://dx.doi.org/10.21037/jphe-20-16). The author has no conflicts of interest to declare.

Ethical Statement: The author is accountable for all aspects of the work in ensuring that questions related to the accuracy or integrity of any part of the work are appropriately investigated and resolved.

References

1. IARC. Diesel and gasoline engine exhausts. In Diesel and Gasoline Engine Exhausts and Some Nitroarenes. IARC Monographs on the Evaluation of Carcinogenic Risk of Chemicals to Humans, vol. 46. Lyon: International Agency for Research on Cancer, 1989.
2. NTP. Report on Carcinogens Background Document for Diesel Exhaust Particulates. Research Triangle Park: National Toxicology Program, 2000.
3. Sturm R. Deposition of diesel exhaust particles in the human lungs: theoretical simulations and experimental data. J Public Health Emerg 2017;1:70.
4. Sturm R. Theoretical deposition of random walk-generated nanoaggregates in the lungs of healthy males and females. J Publ Health Emerg 2018;2:4.
5. Sturm R. Theoretical deposition of diesel exhaust particles in the respiratory tract of children. J Public Health Emerg 2019;3:12.
6. Sturm R. Nanotubes in the respiratory tract - Deposition modeling. Z med Phys 2015;25:135-45.
7. Sturm R. A stochastic model of carbon nanotube deposition in the airways and alveoli of the human respiratory tract. Inhal Toxicol 2016;28:49-60.
8. Sturm R. Spatial visualization of theoretical nanoparticle deposition in the human respiratory tract. Ann Transl Med 2015;3:326.
9. Sturm R. Inhaled nanoparticles. Phys Today 2016;69:70-1.
10. Groblicki PJ. Particle Size Variation in Diesel Car Exhaust. SAE Technical Paper Series no. 790421. Warrendale: Society of Automotive Engineers, 1979.
11. Ullman TL. Investigation of the Effects of Fuel Composition on Heavy Duty Diesel Engine Emissions. SAE Technical Paper No. 892072. Society of Automotive Engineers, 1989.
12. McClellan RO. Toxicological effects of emissions from diesel engines. Dev Toxicol Environ Sci 1986;13:3-8.
13. Williams RL. Diesel particulate emissions: Composition, concentration, and control. Dev Toxicol Environ Sci 1982;10:15-32.
14. Baumgard KJ, Johnson JH. The effect of Fuel and Engine Design on Diesel Exhaust Particle Size Distributions. SAE Technical Paper Series No. 960131. Warrendale: Society of Automotive Engineers, 1996.
15. Garshick E, Laden F, Hart JE, et al. Lung cancer and vehicle exhaust in trucking industry workers. Environ Health Perspect 2008;116: 1327-32.
16. Neumeyer-Gromen A, Razum O, Kersten N, et al. Diesel motor emissions and lung cancer mortality—results of the second follow-up of a cohort study in potash miners. Int J Cancer 2009;124:1900-6.
17. Penconek A, Arkadiusz M. Deposition of diesel exhaust particles from various fuels in a cast of human respiratory system under two breathing patterns. J Aerosol Sci 2013;63:48-59.
18. Sturm R. Bioaerosols in the lungs of subjects with different ages – Part 2: clearance modeling. Ann Transl Med 2017;5:95.
19. Sturm R. Theoretical deposition of carcinogenic particle aggregates in the upper respiratory tract. Ann Transl Med 2013;1:25.
20. Sturm R. Theoretical models for dynamic shape factors and lung deposition of small particle aggregates originating from combustion processes. Z med Phys 2010;20:226-34.
21. Sturm R. Theoretical deposition of variably sized platelets in the respiratory tract of healthy adults. AME Med J 2018;3:5.
22. Sturm R, Hofmann W. A theoretical approach to the

deposition and clearance of fibers with variable size in the human respiratory tract. J Hazard Mater 2009;170:210-8.
23. Sturm R. Theoretical models for the simulation of particle deposition and tracheobronchial clearance in lungs of patients with chronic bronchitis. Ann Transl Med 2013;1:3.
24. Sturm R. Deposition of ultrafine particles with various shapes in the human alveoli – a model approach. Comp Math Biol 2016;5:4.
25. Hofmann W, Sturm R, Winkler-Heil R, et al. Stochastic model of ultrafine particle deposition and clearance in the human respiratory tract. Radiat Prot Dosimetry 2003;105:77-80.
26. Sturm R. Theoretical and experimental approaches to the deposition and clearance of ultrafine carcinogens in the human respiratory tract. Thorac Cancer 2011;2:61-8.
27. Sturm R. Theoretical approach to the hit probability of lung-cancer-sensitive epithelial cells by mineral fibers with various aspect ratios. Thoracic Cancer 2010;1:116-25.
28. Sturm R. Modeling the deposition of bioaerosols with variable size and shape in the human respiratory tract – A review. J Adv Res 2012;3:295-304.
29. Sturm R. Inhalation of nanoplatelets- theoretical deposition simulations. Z med Phys 2017;27:274-84.
30. Hofmann W, Sturm R. Stochastic model of particle clearance in human bronchial airways. J Aerosol Med 2004;17:73-89.
31. Sturm R. A three-dimensional model of tracheobronchial particle distribution during mucociliary clearance in the human respiratory tract. Z Med Phys 2013;23:111-9.
32. Sturm R, Hofmann W. Mechanistic interpretation of the slow bronchial clearance phase. Radiat Prot Dosimetry 2003;105:101-4.
33. Sturm R. Theoretical simulation of diesel exhaust particle clearance from the human respiratory tract. J Public Health Emerg 2017;1:74.
34. Sturm R. A computer model for the clearance of insoluble particles from the tracheobronchial tree of the human lung. Comput Biol Med 2007;37:680-90.
35. Sturm R, Hofmann W. A multi-compartment model for slow bronchial clearance of insoluble particles—extension of the ICRP human respiratory tract models. Radiat Prot Dosimetry 2006;118:384-94.
36. Sturm R, Hofmann W. Stochastic modeling predictions for the clearance of insoluble particles from the tracheobronchial tree of the human lung. Bull Math Biol 2007;69:395-415.
37. Sturm R. Modeling bronchial clearance in the lungs of healthy subjects and smokers. Comp Math Biol 2017;6:2.
38. Sturm R, Hofmann W, Scheuch G, et al. Particle clearance in human bronchial airways: Comparison of stochastic model predictions with experimental data. Ann Occup Hyg 2002;46:329-33.
39. Sturm R. Modeling the delay of mucous flow at the carinal ridges of the human tracheobronchial tree. Comp Math Biol 2014;3:6.
40. Hofmann W, Sturm R, Asgharian B. Stochastic simulation of particle clearance in human bronchial airways. J Aerosol Sci 2001;2S807-8.
41. Svartengren M, Svartengren K, Europe E, et al. Long-term clearance from small airways in patients with chronic bronchitis: experimental and theoretical data. Exp Lung Res 2004;30:333-53.
42. Sturm R. An advanced mathematical model of slow bronchial clearance in the human respiratory tract. Comp Math Biol 2016;5:2.
43. Sturm R. An advanced stochastic model for mucociliary particle clearance in cystic fibrosis lungs. J Thorac Dis 2012;4:48-57.
44. Sturm R. Theoretical models of carcinogenic particle deposition and clearance in children's lungs. J Thorac Dis 2012;4:368-76.
45. Sturm R. Age-dependence and intersubject variability of tracheobronchial particle clearance. Pneumon 2011;4:77-84.
46. International Commission on Radiological Protection (ICRP). Human respiratory tract model for radiological protection, Publication 66. Oxford: Pergamon Press, 1994.
47. Sturm R. Theoretical deposition of nanotubes in the respiratory tract of children and adults. Ann Transl Med 2014;2:6.
48. Sturm R. Computer-aided generation and lung deposition modeling of nano-scale particle aggregates. Inhal Toxicol 2017;29:160-8.
49. Sturm R. A computer model for the simulation of fiber-cell interaction in the alveolar region of the respiratory tract. Comput Biol Med 2011;41:565-73.
50. Sturm R, Hofmann W. A computer program for the simulation of fiber deposition in the human respiratory tract. Comput Biol Med 2006;36:1252-67.

doi: 10.21037/jphe-20-16
Cite this article as: Sturm R. Modeling tracheobronchial clearance of nanoparticles with variable size and geometry. J Public Health Emerg 2021;5:12.